ORIGINAL PAPER

Assessment of regional drought risk coupled with drought response capacity considering water supply systems

Ji Eun Kim[1] · Joo-Heon Lee[2] · Tae-Woong Kim[3]

Abstract

Drought is a complex combination of natural, physical, and social phenomena. Prolonged drought can result in significant socioeconomic damage. Because the impact of drought varies according to the regional ability to cope with drought, it is necessary to assess the risk of drought by considering regional impact and response capacity. This study aims to improve the conventional drought risk (CDR) assessment method, which typically combines drought hazard and drought vulnerability. We proposed a modified drought risk (MDR) assessment that couples the regional response capacity with the local water supply system, in addition to drought hazard and vulnerability. The application results for South Korea indicated that the MDR coupled with regional response capacity (MDR-RC) was high in the central and northeastern regions, whereas the CDR was high in the southwest regions. A comparison of the regions characterized by high MDR-RC and those that experienced actual drought events and took measures in response indicated that MDR-RC will be useful in drought planning and risk-based decision-making.

1 Introduction

Drought is generally defined as a recurring phenomenon caused by a long-term lack of precipitation, leading to water shortages (Zhao et al. 2020). Because droughts progress gradually over extended periods, they can affect ecosystems, agriculture, human society, and economies. Drought is typically classified as meteorological, agricultural, hydrological, or socioeconomic. However, each type of drought occurs in a particular sequence or in combination. Drought is influenced by a range of climate-related factors, including rainfall, evapotranspiration, and temperature, as well as human-induced changes in hydrological processes and physical environments (Van Loon et al.

2016; Frischen et al. 2020). In addition, because the impacts of drought are often complex, indirect, and invisible, identifying the causes and effects of drought can entail significant efforts.

In general, risk is described as the possibility of adverse consequences or expected losses resulting from interactions between hazards and vulnerable conditions (Wilhite 2000). Being defined as the potential losses from a particular hazard imposed by a drought event (Brooks et al. 2005; Cardona et al. 2012), drought risk is quantified by the product of the probability of drought occurrence and the negative consequences from the drought. Drought risk is often driven by and comes from interactions among a variety of context- and impact-specific factors, including environmental, social, economic, cultural, physical, and/or governance-related aspects (Birkmann et al. 2013). Drought risk consists of hazard (i.e., the probability of drought occurrence), vulnerability (i.e., the sensitivity of regional system affected by drought), and response capacity (i.e., the ability to cope with drought). Because drought risk varies greatly depending on the combination of these factors, a drought risk assessment is essential to

✉ Tae-Woong Kim
twkim72@hanyang.ac.kr

[1] Research Institute of Engineering Technology, Hanyang University, Ansan 15588, Korea

[2] Department of Civil Engineering, Joongbu University, Goyang 10279, Korea

[3] Department of Civil and Environmental Engineering, Hanyang University, Ansan 15588, Korea

understand and reduce the negative impacts of a drought (Hagenlocher et al. 2019).

Studies of drought risk have been conducted around the world, and the basic framework for assessing drought risk is relatively well developed. Nasrollahi et al. (2018) attempted to identify the spatial and temporal patterns of drought hazard and risk in Semnan province, Iran, using a conceptual framework that combines hazard and vulnerability. Yu et al. (2021) employed principal component analysis (PCA) to aggregate a drought vulnerability index (DVI) using multiple socio-economic indicators, performed copula-based drought frequency analysis to calculate a drought hazard index (DHI), and multiplied the DVI by the DHI to produce a drought risk index (DRI). These drought risks are typically assessed by combining only drought hazard and vulnerability, as it is difficult to incorporate drought response capacity into a drought risk framework (Dabanli 2018; Nasrollahi et al. 2018; Buurman et al. 2020; Zhao et al. 2020; Yu et al. 2021).

Drought is closely related to the availability of water resources and has a significant impact on the water supply in a region. If a drought continues, damages that people can feel directly such as restrictions on drinking water, agricultural and industrial water, and hydroelectric power generation. However, drought damage may differ across a region depending on the ability to supply water. It is therefore necessary to determine the water supply capacity when assessing drought risk through the drought response capacity of the region.

Studies conducted in Korea have demonstrated that drought risk analysis without considering the water supply system can yield different results from the actual damage (Kim et al. 2015; Yu et al. 2021). This is because many regions in Korea rely on regional and municipal systems for their water supply. Drought-affected regions where people suffer from water shortages are directly related to water supply. In this study, we assessed the drought risk in two ways: by considering drought hazard and vulnerability, i.e., the conventional drought risk (CDR), and by modifying CDR coupled with the response capacity (MDR-RC). The latter presents the potential impact associated with water supply and demand that results from drought in a region. An assessment of the MDR-RC must therefore consider the regional water supply system.

Most studies related to water supply systems evaluate only the water supply capacity, which has not been linked to the drought risk framework. For example, Nam et al. (2015) applied an assessment model of irrigation vulnerability to predict the impacts of agricultural water demand and supply on reservoir operations. The model evaluated the performance of water supplies in agricultural reservoirs in governing local water management decisions. Murgatroyd et al. (2022) developed a coupled simulation model combining climate simulations, hydrological models, and water resource systems at a national scale. To explore the effectiveness of strategic water supplies, they demonstrated how extreme meteorological droughts propagated into hydrological droughts and water shortages. Choi et al. (2022) developed a framework for calculating the available days of water supply from upstream intakes using a soil and water assessment tool. However, an evaluation of water supply capacity that is not linked to a drought risk framework will not accurately represent the drought risk because it does not account for the actual regional drought occurrence and water resources conditions. Thus, it is necessary to assess drought hazard, vulnerability, and response capacity together for a comprehensive drought risk assessment.

Although not directly connected to water supply, drought vulnerability assessment is important as drought vulnerability indicates the negative impact of drought on the socioeconomic sectors of region. Drought vulnerability assessment is also useful in planning policy measures to reduce drought damage (Rajsekhar et al. 2015). In addition, droughts with higher socioeconomic vulnerability are expected to cause more losses (Mishra and Singh 2010).

As a vulnerability assessment integrates various socioeconomic factors, it focuses on how to weigh the factors. Equal weights are widely used to exclude the subjective elements of surveys. However, they cannot incorporate the contribution of each indicator to a vulnerability index. Recently, various statistical methods have been used to secure the objectivity of factor weights and include the contribution of indicators to the vulnerability. Yu et al. (2021) used principal component analysis (PCA) to aggregate a drought vulnerability index (DVI) using multiple socioeconomic indicators and copula-based drought frequency analysis to calculate a drought hazard index (DHI) that considers the occurrence probability of meteorological drought. Zhou et al. (2022) applied an entropy fuzzy pattern recognition model to quantitatively evaluate regional agricultural drought vulnerability and deal effectively with the fuzziness and randomness between evaluation samples and evaluation grades. Kim et al. (2021) evaluated the performance of PCA, a Gaussian mixture model (GMM), and the equal-weighting method to objectively determine the weights of drought vulnerability factors.

To summarize, most previous research efforts separated drought risk assessment from water supply capacity assessment. Drought response capacity is a key factor in mitigating drought risk, but often focuses on finances, governance, and policy, rather than hydrological capacity. Water supply capacity is rarely included in drought risk assessments. Considering people feel drought impacts when water supply fails, CDR does not appropriately

reflect the drought impact or damage in the region, as well as the response capacity to drought.

It is increasingly understood that drought risk assessment should be tailored to the needs of specific users so that management plans can be developed to reduce impacts (Vogt et al. 2018). In this study, we evaluate MDR-RC by synthesizing drought risk, vulnerability, and drought response capacity considering local water supply systems. This can quantify drought damage, impact, and risk in the region. MDR-RC is the risk that people actually feel beyond the combining of drought hazard and vulnerability for the CDR. It integrates drought hazard due to water supply failures, drought vulnerability, and the capacity to respond to water supply failures. The final purpose of this study is to assess regional drought risks based on the MDR-RC and compare the performance with the CDR.

2 Study area and data collection

South Korea covers 100,210 km^2 of Northeast Asia (33–38 °N and 126–131 °E; Fig. 1) and has a population of 51.47 million people. The average annual precipitation is 1270 mm and the average annual temperature is 13.2 °C. The climate of South Korea is strongly influenced by the Asian monsoon, with an average annual temperature of 13.2 °C. As two-thirds of the annual rainfall is concentrated in summer, from late June to early September, severe droughts are likely to occur in the rest of the year (i.e., from autumn to the next spring) (Yoo et al. 2015). During the past 30 years, South Korea suffered from severe droughts at least once every 5–8 years, and moderate droughts have happened annually in regional and national scales since 1990 (Bae et al. 2018). For this reason, the necessity for drought risk assessment is increasing. This study assessed the regional drought risk of 160 administrative districts in South Korea, as shown in the right panel of Fig. 1.

To assess drought risk, we selected indicators appropriate for the purposes of the study and the concepts of drought hazard, vulnerability, response capacity, and risk. Terms related to drought risk assessment were defined based on various references and the universally quoted Intergovernmental Panel on Climate Change (IPCC 2014). After reviewing previous studies and considering the ease of data collection, we selected non-redundant evaluation indicators. For the CDR, drought hazard is a meteorological aspect of drought occurrence probability, and drought vulnerability is a socioeconomic aspect of the regional systems that are negatively associated with drought. Daily precipitation data from 1973 to 2019 provided by the Korea Meteorological Administration were used to assess the drought hazard. The drought vulnerability indicators selected for the study were population, area, farm population, agricultural land area, area of industrial complexes, amount of domestic water usage, amount of agricultural water usage, amount of industrial water usage, daily water supply per capita, and water supply ratio. For the MDR-RC, drought hazard is the probability of the occurrence of a water supply failure, drought vulnerability is the socioeconomic sensitivity for the regional system to adversely affect or receive during the drought, and drought response capacity is the regional water supply capacity that can mitigate the impact of drought. Accordingly, drought hazard was assessed based on discharge data for calculating the water deficiency. Unlike drought vulnerability of CDR, drought vulnerability assessment indicators were selected to provide a detailed understanding of vulnerability, excluding water usage. The selected indicators included population, farm population, recipients of basic living, solitary senior citizens, total area of the district, agricultural area, area of industrial complex, ratio of water leakage, daily water supply per capita, and water supply ratio. For the response capacity, dams, reservoirs, groundwater, and water intake related to water supply and demand were used (Table 1).

Considering the temporal range, period, and update interval of the data, the temporal resolution of the evaluation indicators was set on an annual basis from 2001 to 2019. The spatial range of data was set for 160 administrative districts. These indicators were collected from water supply statistics, National Statistical Office and Water Resources Management Information System.

3 Methodology

3.1 Drought hazard index

Drought hazard, the probability of the occurrence of drought, is commonly quantified using a drought index. Among various drought indices used for drought monitoring and risk assessments in South Korea (Kim et al. 2014, 2020; Azam et al. 2018; Yu et al. 2021), we chose the standardized precipitation index (SPI-6) for CDR and the joint management drought index (JMDI) for MDR-RC.

The SPI is widely used to determine the drought hazard by fitting and transforming long-term precipitation series into a normal distribution. The SPI can be computed at different time scales. Short-term (e.g., 1 month, 3 months) accumulation periods are generally used for identifying meteorological droughts and whereas long-term (more than 3 months) accumulation periods are considered to identify agricultural and hydrological droughts. In this study, the six-month SPI(SPI-6) was used for CDR, because it fits well with the dry and wet conditions in South Korea and has been successfully applied to drought monitoring (Kim
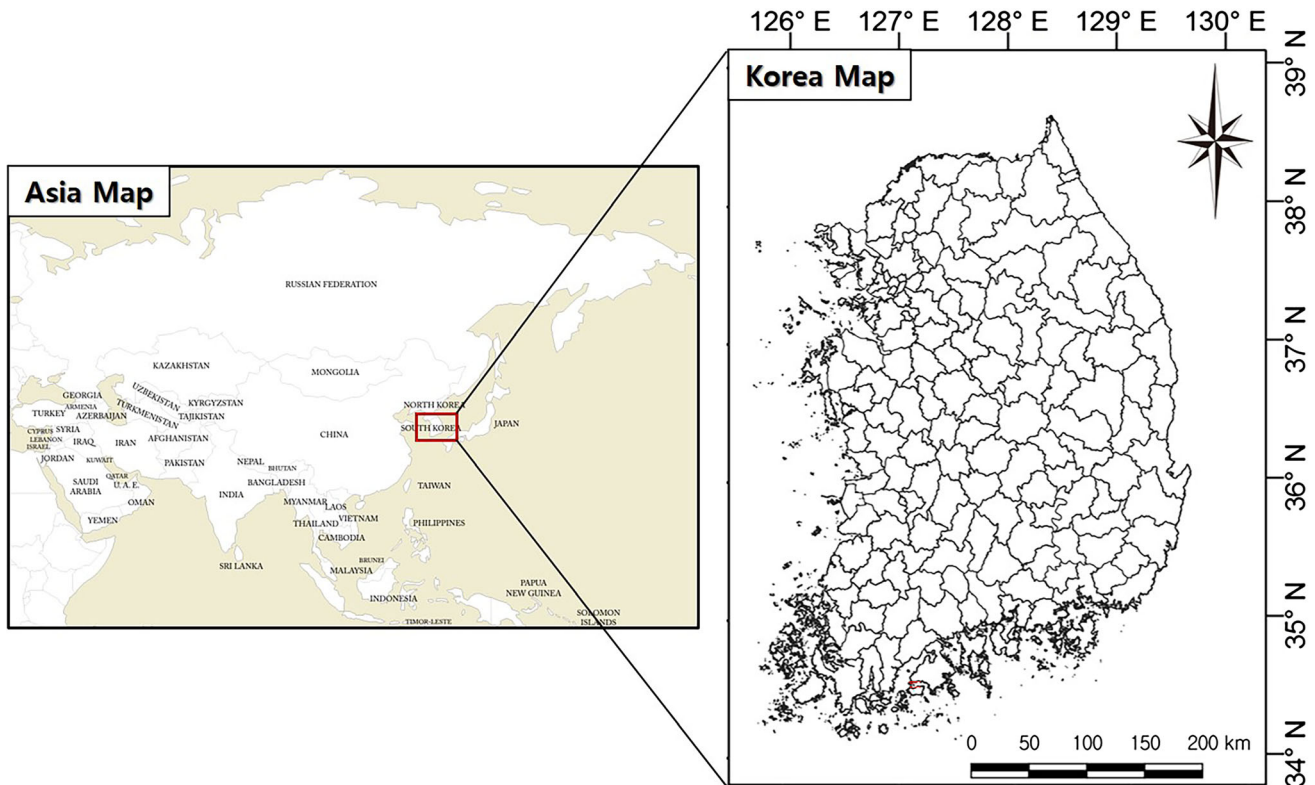
Fig. 1 Map of the study area

Table 1 Indicators for drought response capacity

Id	Indicator		Id	Indicator
I1	Water resources retention	Dam	I13	Amount of agricultural water usage
I2		River	I14	Amount of groundwater usage
I3		Reservoir	I15	Potential groundwater development
I4		Groundwater	I16	Ratio of sewage reuse
I5	Water intake	Regional dam	I17	Amount of sewage treatment
I6		Local dam	I18	Amount of rainwater reuse
I7		Surface water	I19	Effluents of sewage treatment
I8		Subsurface water	I20	Amount of sewage inflow
I9		Reservoir	I21	Area
I10		Groundwater	I22	Annual precipitation
I11	Amount of domestic water usage		I23	Population
I12	Amount of industrial water usage		I24	Water supply ratio

et al. 2014; Azam et al. 2018), and represents different attributes of droughts in terms of duration, magnitude, intensity, and consequently manifest the hazard (Yu et al. 2021). A drought event is identified by the SPI consecutively lower than –1.0. After calculating the drought duration and magnitude for individual events, the optimal marginal distributions of duration and magnitude were determined based on a Kolmogorov–Smirnov test. Using Archimedean copula functions such as Clayton, Frank, and Gumbel, as given in Eq. (1), the joint probability distribution was estimated. A drought hazard index of CDR (DHI_{CDR}) was determined by applying the ranking method and considering the drought frequency and severity developed by Yu et al. (2021). The nine classes of drought severity were ranked, and their weights were determined by rank, which ranged from zero to unity, as described in

Table 2 (Yu et al. 2021). The DHI$_{CDR}$ was calculated by weighting the probability of occurrence of each drought class as expressed in Eq. (2).

$$F(x, y) = C(F_X(x), F_Y(y)) \tag{1}$$

$$DHI_{CDR} = \sum_{k=1}^{rank} r_k f(d_k, m_k) \tag{2}$$

where $F_X(x)$ and $F_Y(y)$ are the marginal distributions of duration and magnitude, respectively, r_k is the weight of the k th drought stage, and $f(d_k, m_k)$ is the occurrence probability of drought with duration (d_k) and intensity (m_k).

The drought hazard of MDR-RC indicates the possibility of water supply failure, and can be quantified by the JDMI, which was developed by Yu et al. (2019) to quantify the potential occurrence of water supply failure. If the drought hazard of MDR-RC is assessed with streamflow data, the results can be distorted by regional differences in the presence or absence of observed streamflow, i.e., the probability of drought occurrence can be overestimated in regions that have low average streamflow, short-period data, or no observation points. The JDMI can overcome these limitations and calculate the probabilistic possibility of water supply failure. The JDMI combined the probability that the water system can normally supply water during a specific planned period (i.e., reliability) and the quantitative risk of water shortage (i.e., volumetric failure). The water supply safety indicators were calculated for a certain operation period of the water supply facility. In this study, the data period (2001–2019) was divided to determine the water supply safety of the water system over time using a five-year moving window (MV), i.e., MV1(2001–2005), MV2(2002–2006), and so on. The joint cumulative distribution function (JCDF) is expressed using the copula of two random variables (i.e., the reliability of water supply and the risk of water shortage), and the JDMI can produce an estimate by reducing the information of the multi-dimensional JCDF into one-dimension using a Kendall distribution function. The drought hazard index of MDR-RC (DHI_{MDR-RC}) was calculated using the JDMI by applying the grading method, which takes into account both the

magnitude of drought severity and the frequency of occurrence because it is a function that combines the weight of severity and the rating of the associated frequency of drought occurrence. Weight scores were determined by considering SPI intervals, such that 1 for normal drought, 2 for moderate drought, 3 for severe drought, 4 for extreme drought, and 0 for wet conditions. Similarly, rating scores were assigned from 1 to 4 in increasing order, dividing the interval of cumulative probabilities in each drought range (Dabanli 2018). This was done using Jenks natural break optimization, which divided the actual occurrence probabilities calculated for all the grids that lie within the same planning region identified by Rajsekhar et al. (2012) into four ratings (Rajsekhar et al. 2015). The DHI_{MDR-RC} was calculated as Eq. (3) and rescaled to the 0–1 range.

$$DHI_{MDR-RC} = (ND_r \times ND_w) + (MD_r \times MD_w) + (SD \times SD_w) + (ED_r \times ED_w) \tag{3}$$

where, ND_r, MD_r, SD_r, and ED_r (ND_w, MD_w, SD_w, and ED_w) refer to the rating (weight) corresponding to normal ($-1.0 < \text{SPI} < 0$), moderate ($-1.5 < \text{SPI} \leq 1.0$), severe ($-2.0 < \text{SPI} \leq 1.5$), and extreme ($\text{SPI} \leq 2.0$) drought, respectively.

3.2 Drought vulnerability index

Drought vulnerability is quantified based on regional socioeconomic data and involves a weighting allocation that integrates various indicators. In this study, the weights of drought vulnerability assessment indicators were calculated by applying entropy, PCA, and GMM methods. Because each method reflects specific information in weighting, it is more appropriate to consider all methods than to adopt one. For the drought vulnerability for CDR and MDR-RC, the integrated weight was calculated by arithmetically averaging the weights of three methods.

Entropy weighting is a method of finding a signal with high cohesion based on the information of a signal and assigning the high weights. The entropy method evaluates

Table 2 Description of drought weights corresponding to ranking

Ranking	Intensity (m_k)	Duration (d_k) (Days)	Weight (r_k)
1	–1.0 (moderate drought)	30	0.1
2		90	0.2
3		120	0.3
4	–1.5 (severe drought)	30	0.4
5		90	0.6
6		120	0.7
7	–2.0 (extreme drought)	30	0.8
8		90	0.9
9		120	1.0

value by measuring the degree of differentiation. The greater the degree of dispersion of the measured value, the greater the degree of differentiation of the index, and more information can be derived (Zhu et al. 2020). The entropy weight for DVI ($w_{j,entropy}$) can be obtained by using the information entropy, as given in Eq. (4).

$$w_{j,entropy} = \frac{1 - E_j}{\sum_{j=1}^{n}(1 - E_j)} \tag{4}$$

$$E_j = -k\sum_{i=1}^{m} P_{ij} \ln P_{ij}, k = \frac{1}{\ln(m)} \, for \, j = 1, 2, \cdots, n. \tag{5}$$

$$P_{ij} = \begin{bmatrix} x_{11} & \cdots & x_{1j} & \cdots & x_{1n} \\ \vdots & \ddots & \vdots & \ddots & \vdots \\ x_{i1} & \cdots & x_{ij} & \cdots & x_{in} \\ \vdots & \ddots & \vdots & \ddots & \vdots \\ x_{m1} & \cdots & x_{mj} & \cdots & x_{mn} \end{bmatrix} \tag{6}$$

where, E_j is the information entropy, P_{ij} is the decision(-correlation) matrix, x_{ij} is the jth indicator of ith region, m is the number of regions, n is the number of regions indicators, respectively.

The $DVI_{entropy}$ is calculated as the weights multiplied by normalized indicators, as described in Eq. (7).

$$DVI_{entropy} = \sum_{j=1}^{n} w_{j,entropy} \times P_{ij} \tag{7}$$

PCA combines various correlated indicators to include as much information as possible and assigns a high weight to indicators with significant information. Each of the correlated indicators (e.g., population, area, and water supply ratio, etc.) that consist of one factor (drought vulnerability) has a different contribution. PCA efficiently recognizes data patterns and minimizes information loss while reducing the high dimensionality of the dataset (Liu and Schisterman 2004). The PCA weight ($w_{j,PCA}$) is determined by combining principal component loadings and variance explanation, as described in Eq. (8).

$$w_{j,PCA} = \frac{c_j v_k}{\sum_{j=1}^{n} c_j v_k} \tag{8}$$

where c_j denotes the principal component loadings of the jth indicator, and v_k is the variance explanation of the kth principal component including the jth indicator.

After creating correlation matrices of the indicators, the principal component loadings and the variance explanation can be calculated by estimating the eigenvalues and eigenvectors (Kim et al. 2021). Principal component scores (weights) of the indicators are determined by combining the loadings and variance explanation, as described in Eq. (8).

The DVI_{PCA} is the sum of the weights multiplied by normalized indicators, as given in Eq. (9).

$$DVI_{PCA} = \sum_{j=1}^{n} w_{j,PCA} \times P_{ij} \tag{9}$$

The GMM method estimates the model parameter using an expectation–maximization (EM) algorithm, in which each indicator has a Gaussian distribution. Because the GMM method is a parametric statistical model that assumes the data originate from a weighted sum of several Gaussian sources, it assigns the weight by estimating the model parameters (Kim et al. 2021). The weights of the GMM ($w_{j,GMM}$) are determined by estimating the model parameter to satisfy Eq. (10):

$$p(\theta|x) = \sum_{j=1}^{n} w_{j,GMM} p(x|\theta_j) \tag{10}$$

where $p(x|\theta_j)$ is the probability density function of the component of a mixed model, θ_j is its respective parameter, and n is the number of Gaussian sources in the GMM equal to the number of indicators (Shental et al. 2004).

In a GMM, it is important to estimate model parameters such as the weight w_j of the jth element to distinguish the categories to which the data belong (Moraru et al. 2019). To estimate the parameters, an EM algorithm alternately applies an expectation step (E-step) of calculating the expectation of the log-likelihood and a maximization step (M-step) of obtaining the variable value that maximizes this expectation. It is possible to draw confidence ellipsoids for multivariate models and compute the Bayesian information criterion (BIC) to evaluate the characteristics of GMM in the indicators (Kim et al. 2021). After determining the weights from the EM algorithm and the BIC, DVI_{GMM} can be calculated as the sum of the weights multiplied by normalized indicators, as described in Eq. (11).

$$DVI_{GMM} = \sum_{j=1}^{n} w_{j,GMM} \times P_{ij} \tag{11}$$

3.3 Drought response capacity index

Because drought response capacity is related to water resources and water supply capabilities of regional systems, it can be quantified using information on regional water resource. However, there is a limit to basing the value of a regional water supply capacity on raw data of the water resource information. Qin and Zhang (2018) established a formula for a supply matching index to measure a regions' ability to provide water resources using water supply, water demand, water utilization rate, and

groundwater. Referring to Qin and Zhang (2018), we introduced the formulas to calculate the drought response capacity based on the water supply capacity in consideration of the regional water supply system and integrated the water supply capacity and various water resources information employing the Bayesian network. Indicators of the drought response capacity are composed largely of water supply capacity, the amount of availability water resources, and ratio of reuse. The amount of available water resources is a measure of regional water resource conditions, which can be calculated using precipitation per capita (i.e., annual precipitation(I22)/population(I23)) and potential groundwater development per capita (i.e., potential groundwater development(I15)/population(I23)). The ratio of reuse can be calculated by considering the ratio of effluents of sewage treatment (effluents of sewage treatment(I19)/amount of sewage inflow(I20)), sewage reuse (I16), and rainwater reuse (amount of rainwater reuse(I18)/(area(I21)× annual precipitation(I22))).

Water supply capacity (WSC) is based on the amount of water supply and the amount of water usage in the region (Qin and Zhang 2018), as given in Eqs. (12)–(16).

$$WSC = \left\{ (WS_{dam} + WS_{river} + WS_{reservoir}) \times WSR + WS_{ground} \right\} \times \frac{\int_{district} WI}{\int_{region} WI} \tag{12}$$

$$WS_{dam} = \frac{WR_{dam}}{WU_{domestic} + WU_{industrial}} \times \frac{WI_{dam}}{\int_{district} WI} \tag{13}$$

$$WS_{river} = \frac{WR_{river}}{WU_{domestic} + WU_{industrial}} \times \frac{WI_{river}}{\int_{district} WI} \tag{14}$$

$$WS_{reservoir} = \frac{WR_{reservoir}}{WU_{agricultural}} \times \frac{WI_{reservoir}}{\int_{district} WI} \tag{15}$$

$$WS_{ground} = \frac{GW}{WU_{ground}} \times \frac{WI_{dam}}{\int_{district} WI} \tag{16}$$

where WS_{dam}, WS_{river}, $WS_{reservoir}$, and WS_{ground} are the water stress that represents the ratio of retention to water usage corresponding to dam, river, reservoir, and ground, respectively. WR_{dam}, WR_{river}, and $WR_{reservoir}$ are the water retention of dam, river, and reservoir, and $WU_{domestic}$, $WU_{industrial}$, $WU_{agricultural}$, and WU_{ground} are the amounts of usage of domestic water, industrial water, agricultural water, and groundwater, respectively. GW is the amount of groundwater. WI represents the amount of water intake by each type of water retention, $\int_{district} WI$ is the total amount of water intake of the district and $\int_{region} WI$ is the total amount of water intake of the region. WSC is the water supply capacity and WSR is the water supply ratio. Applying the water intake ratio and the water supply rate

allowed us to consider the dependence of the region on the source of water intake or water supply.

The indicators were integrated into drought response capacity index (DRCI) using a Bayesian network (Fig. 2). The Bayesian network consisted of nodes representing various variables and arcs representing dependencies between variables. the causal relationships between nodes were represented by probability information, as given in Eq. (17).

$$P(Z|Y) = \frac{P(Z)P(Y|Z)}{P(Y)} = \frac{P(Z = z, Y = y)}{P(Y = y)} \tag{17}$$

where $P(Z)$ is the prior probability, $P(Z|Y)$ is the posterior probability, and $P(Y)$ is the marginal distribution.

Among inference algorithms such as likelihood weighting, rejection sampling, and Gibbs sampling, likelihood weighting is often applied because it is simple to use and can estimate the posterior probability even in a continuous probability distribution. Assuming that the converging network consists of Y and Z, the likelihood-weighting method only samples the non-evidence variables while fixing the values of the evidence variables (Russell and Norvig 2009). In general, the prior probability is estimated using empirical values or observations.
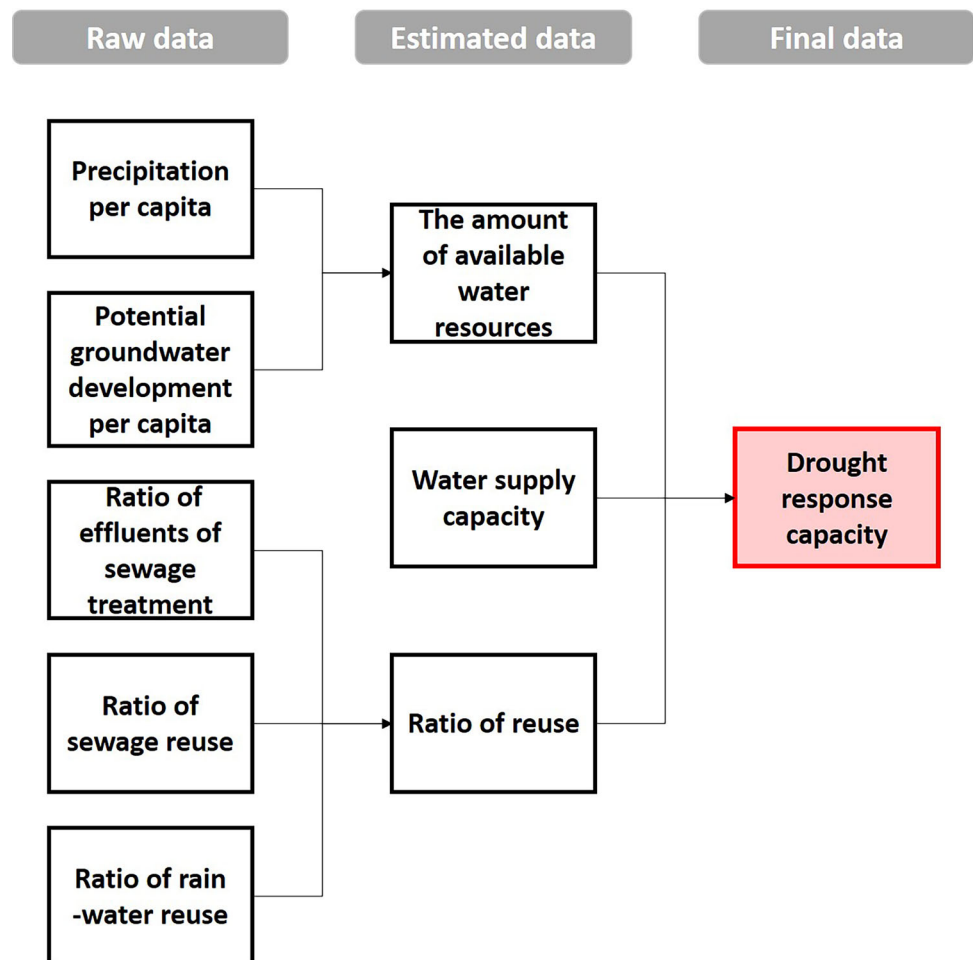
3.4 Drought risk assessment

In this study, the drought risk is defined as the potential damage linked with the water supply and demand that may be occurred by drought in a specific region. It generally quantifies the impact of meteorological drought. However, MDR-RC refers to the impact of the failure of water supply. CDR can be characterized by combining drought hazard and vulnerability, and MDR-RC includes the response capacity to hazard and vulnerability. In practice, it is appropriate that the components of risk are geometrically averaged because they have multiplicative effects on the drought risk. In this study, the drought risk index for CDR (DRI_{CDR}) was calculated by multiplying a root of DHI_{CDR} and DVI_{CDR} as given in Eq. (18). In addition, DRI_{MDR-RC} was calculated by multiplying a cubic root of DHI_{MDR-RC}, DVI_{MDR-RC}, and $DRCI_{MDR-RC}$, where $DRCI_{MDR-RC}$ was modified as shown in Eq. (19) due to the opposite nature of risk, unlike hazard and vulnerability.

$$DRI_{CDR} = DHI_{CDR}^{1/2} \times DVI_{CDR}^{1/2} \tag{18}$$

$$DRI_{MDR-RC} = DHI_{MDR-RC}^{1/3} \times DVI_{MDR-RC}^{1/3} \times (1 - DRCI)^{1/3} \tag{19}$$

As the drought risk can be affected by two or three factors, it was assessed by multiplying all the factors. Drought hazard, vulnerability, response capacity, and risk all have values ranging from 0.00 to 1.00. In addition,

Fig. 2 Bayesian network model for drought response capacity index

drought hazard, vulnerability, and risk, except for response capacity, mean that the closer to 1.00, the more dangerous the situation is, and the closer to 0.00, the less dangerous.

4 Results and discussion

4.1 Drought hazard assessment

For the drought hazard of CDR, the SPI-6 was adopted to determine the occurrence probability of meteorological drought. Drought duration and magnitude were calculated based on the SPI-6, and the optimum marginal distributions of duration and magnitude were fitted based on the K-S test for nine probability distributions (exponential, normal, gamma, lognormal, Poison, Weibull, generalized extreme value, generalized Pareto, and Gumbel distributions). The probability of drought occurrence was quantified using a copula function that combines the marginal distribution functions. The DHI_{CDR} based on the ranking method was calculated by applying the joint probability to Eq. (2). Table 3 provides the drought characteristics and Fig. 3a

shows the drought hazard maps of drought hazard of CDR. A gamma distribution was selected as the optimal marginal probability distribution of duration and magnitude, and a Clayton distribution was selected as the optimal joint probability distribution. On average, 35 meteorological droughts occurred in Korea, with an average duration of 2.63 months and an average magnitude of 3.96 months. In particular, there were many droughts with a long average duration and severe magnitude in the southern coastal regions. The DHI was higher than 0.7 in the southern coastal regions, and the highest region was H1 district with 0.79, as shown in Fig. 3a.

For the drought hazard of MDR-RC, the JDMI was used to determine the possibility of water supply failure. Excess water deficiency was calculated by taking the standard of low flow from the daily discharge in the region. When a drought event was identified, the duration and water shortage were calculated as the water supply safety. The JDMI was estimated by employing the water supply safety indicators to the copula and Kendall distribution functions. The DHI_{MDR-RC} was calculated using the grading method as in Eq. (3). Table 4 provides the drought characteristics

Table 3 Summary of Drought characteristics for DHI_{CDR}

	Number of drought event	Average of drought duration	Average of drought severity
Maximum	45	3.56	5.64
Minimum	24	2.03	3.03
Mean	34.56	2.63	3.96
Standard deviation	4.01	0.29	0.52

and water supply factors for DHI_{MDR-RC} and Fig. 3b shows the maps of DHI_{MDR-RC}. For the optimal marginal probability distribution of duration and water shortage, lognormal was mostly adopted. For the joint probability distribution, the Clayton distribution was adopted. On average, 67 hydrological droughts occurred in Korea, with an average duration of 31.89 days and an average water shortage of 2,085.21 cms-day. Most of the water shortages were in central and southwest Korea. Regarding the water supply failure, the average probability of a normal water supply in Korea during the data period was 0.64, and the average resiliency from a water supply failure was 0.04. In this study, the average volumetric failure was 0.32. Similar to the drought characteristics, the DHI was high in the western coastal region, especially highest at 1.00 in H2, H3, H4, H5, H6, and H7 districts. These areas are expected to have a very high risk of water supply failure.

The DHI_{CDR} and DHI_{MDR-RC} results were markedly different because only meteorological drought was different from the drought or hazard of actual water shortage. Because DHI_{CDR} was computed with the precipitation-based SPI, it resembles the spatial distribution of meteorological drought. DHI_{MDR-RC}, by comparison, was calculated from the discharge-based JDMI, which is similar to the spatial distribution of hydrological drought. Kim et al. (2015) assessed the drought hazard using the effective drought index as the hydrological drought index. The results were similar to what DHI_{MDR-RC}, the hydrological drought index of this study, found. Water in Korea is primarily taken from rivers and dams. The JDMI is useful for catching water supply failure events where the streamflow is below the streamflow requirement. It can be compared to the number of drought forecasts and warnings of actual water supply problems. The issued number of drought forecasts and warnings is shown in Fig. 4. The DHI_{MDR-RC} captured the regions where the drought damage occurred. Many of the forecasts and warnings were issued in the west and southeast coastal areas, where DHI_{MDR-RC} was high. In conclusion, it is difficult to identify regions where water supply failures occur based on precipitation alone. Precipitation cannot be controlled by humans except by monitoring. Flow-based water supply can be controlled by

national policies and plans. DHI_{MDR-RC} can help identify and mitigate drought events related to regional water supply.

4.2 Drought vulnerability assessment

Both drought vulnerabilities of CDR and MDR-RC are associated with regional socioeconomic systems, regardless of drought type. However, the list of indicators will vary according to the research purpose. The objective weighting methods of entropy, PCA, and GMM were employed for the drought vulnerability indicators presented in Sect. 2. Before applying the weighting methods, the standardization was necessary to combine the various socioeconomic indicators with different properties and units into a single index. We used the re-scaling method, which is most suitable when the bounds of the index are known and has the advantage that there are no negative values.

In this study, the weight used for drought vulnerability was obtained by averaging the three weights of entropy, PCA, and GMM. The final weights of the drought vulnerabilities of CDR and MDR-RC are described in Tables 5 and 6. The underlined values in Tables 5 and 6 indicate the highest values in each weight method. The entropy method, considering the degree of diversity for each attribute, produced high estimates in GV2 and WV2 for the drought vulnerabilities of CDR and MDR-RC, respectively. PCA based on the information of indicators produced results that were high in GV7 and WV2 for the drought vulnerabilities of CDR and MDR-RC, respectively. The GMM method, based on the contribution of the distribution of indicators, was high in GV4 and WV8 for the drought vulnerabilities of CDR and MDR-RC, respectively. Because each weighting method has a distinct way of assigning importance, the weights were slightly different. The final weights of averaging integrated each weight were calculated to comprehensively consider these contents, and the results of the drought vulnerabilities of CDR and MDR-RC were calculated to be high at GV7 and WV9, respectively. In the DVI_{CDR}, the weights of agricultural factors were high, whereas, in the DVI_{MDR-RC}, the weights

Fig. 3 Drought hazard map.
a DHI_{CDR}, **b** DHI_{MDR-RC}
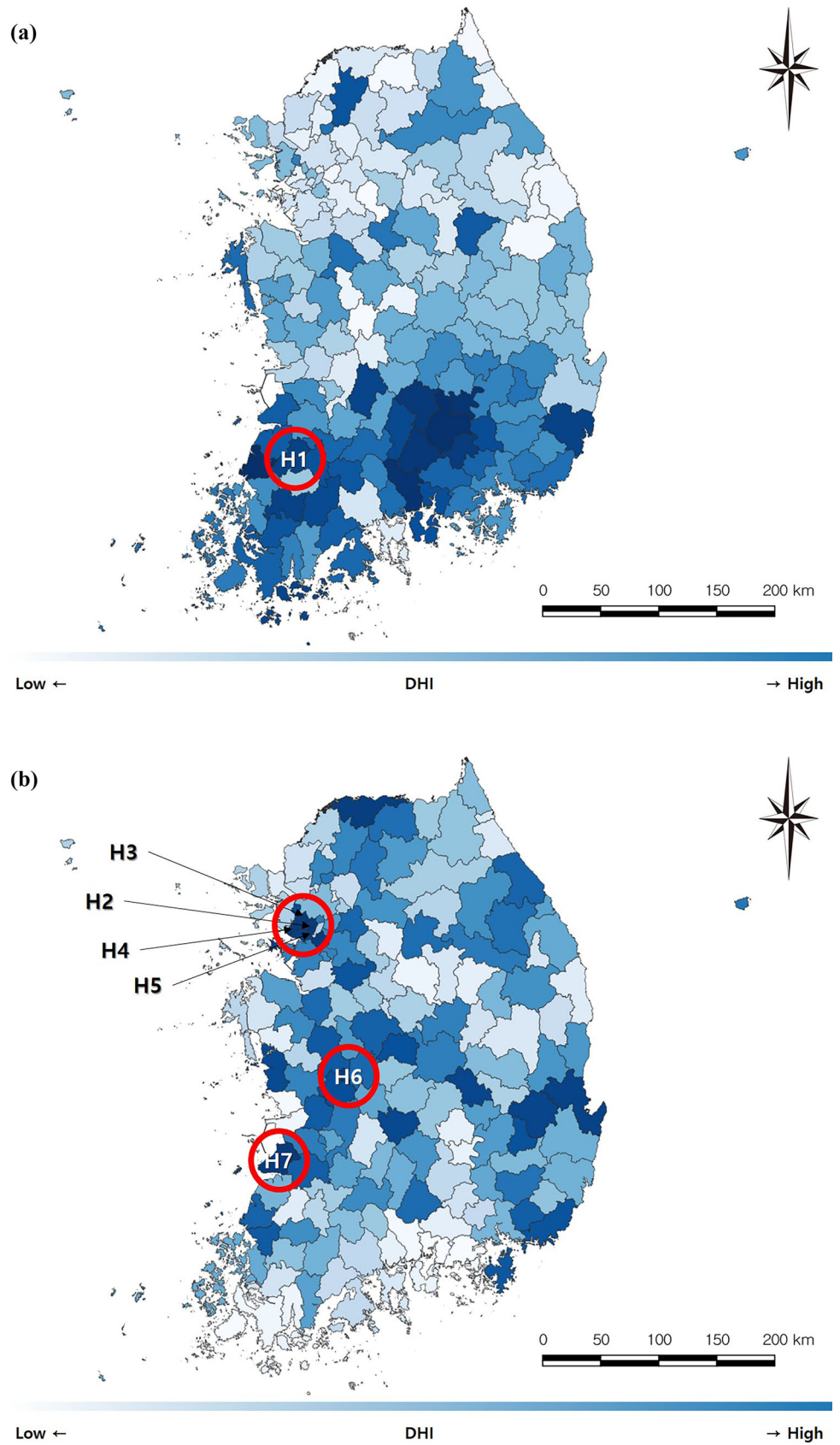
Table 4 Drought characteristics and water supply safety factors for DHI_{MDR-RC}

	Number of drought event	Average of drought duration	Average of water deficiency	Reliability	Resilience	Volumetric failure
Maximum	157	176.71	226,745.57	0.98	0.12	1.19
Minimum	12	8.29	0.05	0.03	0.01	0.04
Mean	66.76	31.89	2,085.21	0.64	0.04	0.32
Standard deviation	30.04	21.65	15,805.75	0.19	0.02	0.21

Fig. 4 Drought forecasts and warnings
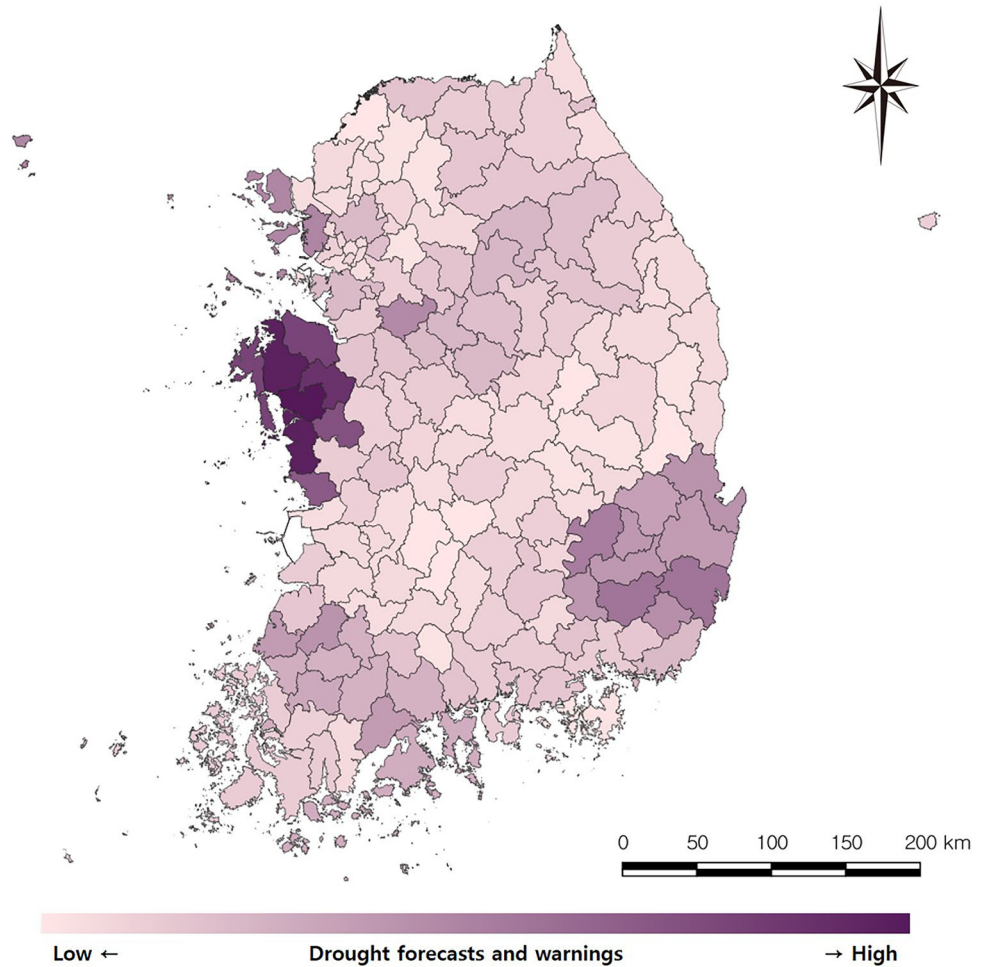
of water supply factors were high. The results of applying the final weights to each indicator are shown in Fig. 5. The DVI_{CDR} was high in the V1 district, an agricultural area, and the DVI_{MDR-RC} was high in the V2 district, where the unit water supply was low. However, the overall results of both drought vulnerabilities were generally high in the central regions. Although the drought vulnerabilities assessed by the DVI_{MDR-RC} and Kim et al. (2015) differed in detail, they were apparently vulnerable in the mid-west regions. As the vulnerability characteristics of the region

were similar, the results of two vulnerabilities resembled each other. However, unlike the DVI_{CDR}, vulnerable information on water usage was not dealt with in the DVI_{MDR-RC}, so slightly different results were confirmed depending on indicators. The results were similar because more urbanized areas had larger agricultural and industrial populations, which reduced the role of weights. To decrease this effect in the future, we plan to analyze the results using a ratio of the indicators, which will give a distinct spatial distribution. Drought vulnerability

Table 5 Weights of indicators for CDR

Indicators		Entropy	PCA	GMM	Final weights
GV1	Population	0.08	0.03	0.14	0.08
GV2	Area	<u>0.14</u>	0.14	0.08	0.12
GV3	Farm population	0.14	0.16	0.12	0.14
GV4	Agricultural land area	0.13	0.18	<u>0.15</u>	0.15
GV5	Area of industrial complex	0.06	0.04	0.03	0.05
GV6	Amount of domestic water usage	0.11	0.01	0.04	0.05
GV7	Amount of agricultural water usage	0.12	<u>0.21</u>	0.12	<u>0.16</u>
GV8	Amount of industrial water usage	0.04	0.02	0.14	0.06
GV9	Daily water supply per capita	0.07	0.06	0.07	0.06
GV10	Water supply ratio	0.10	0.14	0.11	0.12

Table 6 Weights of indicators for MDR-RC

Indicators		Entropy	PCA	GMM	Final weights
WV1	Population	<u>0.08</u>	0.04	0.15	0.09
WV2	Farm population	0.14	0.14	0.10	0.13
WV3	Recipients of basic living	0.08	0.01	0.14	0.07
WV4	Solitary senior citizen	0.10	0.05	0.11	0.09
WV5	Total area of district	0.14	0.14	0.04	0.11
WV6	Agricultural area	0.13	0.13	0.00	0.09
WV7	Area of industrial complex	0.05	0.03	0.13	0.07
WV8	Ratio of water leakage	0.13	0.16	<u>0.15</u>	0.14
WV9	Daily water supply per capita	0.07	<u>0.24</u>	0.10	<u>0.15</u>
WV10	Water supply ratio	0.09	0.07	0.07	0.07

determines the magnitude of damage in the event of a drought. It is difficult to validate with current damage and impact information of drought. The results were significant in prioritizing high-vulnerable areas and identifying indicators that are more likely to be affected.

4.3 Drought response capacity assessment

In assessing the drought risk of MDR-RC, it is important to identify the regional water supply system and determine the drought response capacity. In this study, the regional water supply networks were identified, and the corresponding indicators were recalculated to estimate the DRCI, which implied the region's water supply capacity to mitigate the effects of drought. The regional water supply system can be displayed in a diagram, as shown in Fig. 6, considering water sources such as rivers, dams, and reservoirs and the water supply network. The water supply capacity was calculated by applying the intake source, intake ratio, and water supply ratio to Eqs. (12)–(16) through the regional water supply system. As shown in Fig. 2, the DRCI was determined by consolidating the water supply capacity, the amount of availability water resources, and the ratio of reuse with the Bayesian network. Assuming a normal distribution, the prior probability

distribution reflected the latest information for the region. The posterior probability distribution was inferred by combining the latest information with other years and will be updated as more information is added.

Standardization is necessary for combining the indicators within the Bayesian network. Because the Bayesian network was based on a normal distribution, a standard normalization was applied to unify the range of the indicators with different units by excluding outliers with 95% confidence intervals. The estimated probability distribution was applied to the Bayesian network model to determine the DRCI, and it was standardized to indicate that values closer to 0.00, unlike the DHI and DVI, are the worst.

As shown in Fig. 7, the response capacity was low in the southeast regions, meaning that it would be difficult to recover from a drought. In particular, RC1, RC2, and RC3 districts had the lowest response capacity, and these regions had low water supply capacities. The central region was irrigated by dams, but there was always a shortage of storage of dams, and drought damage was frequent. The southeastern region took most of its water from rivers, but its capacity was low due to the lack of abundant river flow. Based on the comparison, it can be confirmed that RC4, RC5, and RC6 districts had the best response capacity, and the water supply and the ratio of reuse were acceptable.

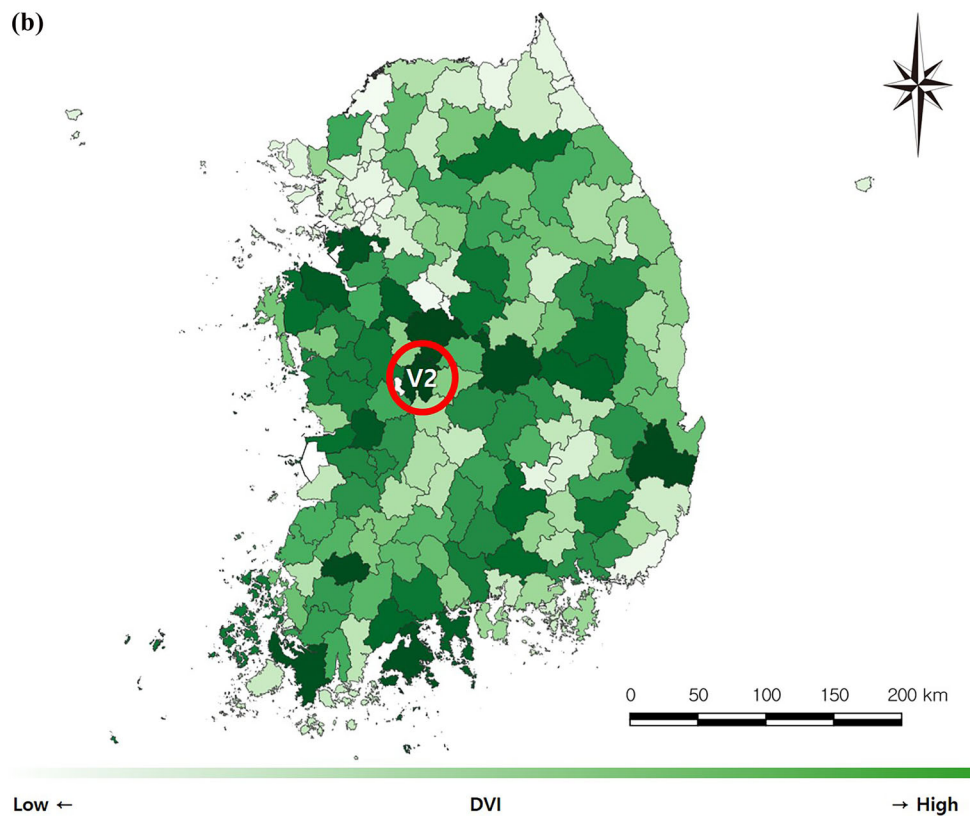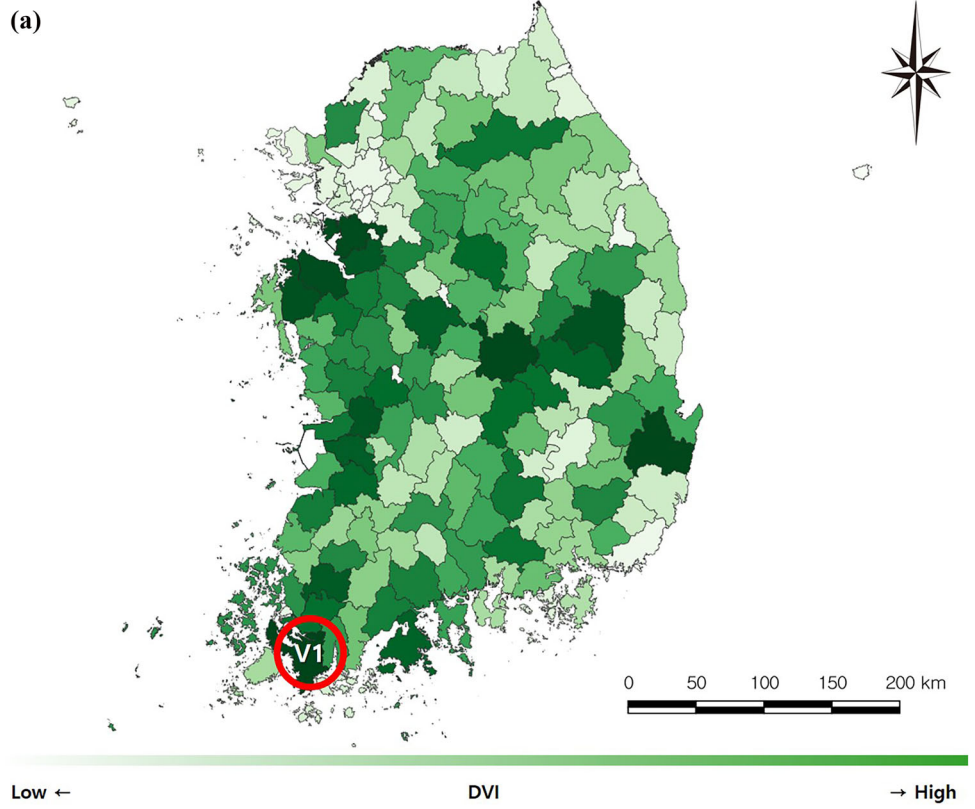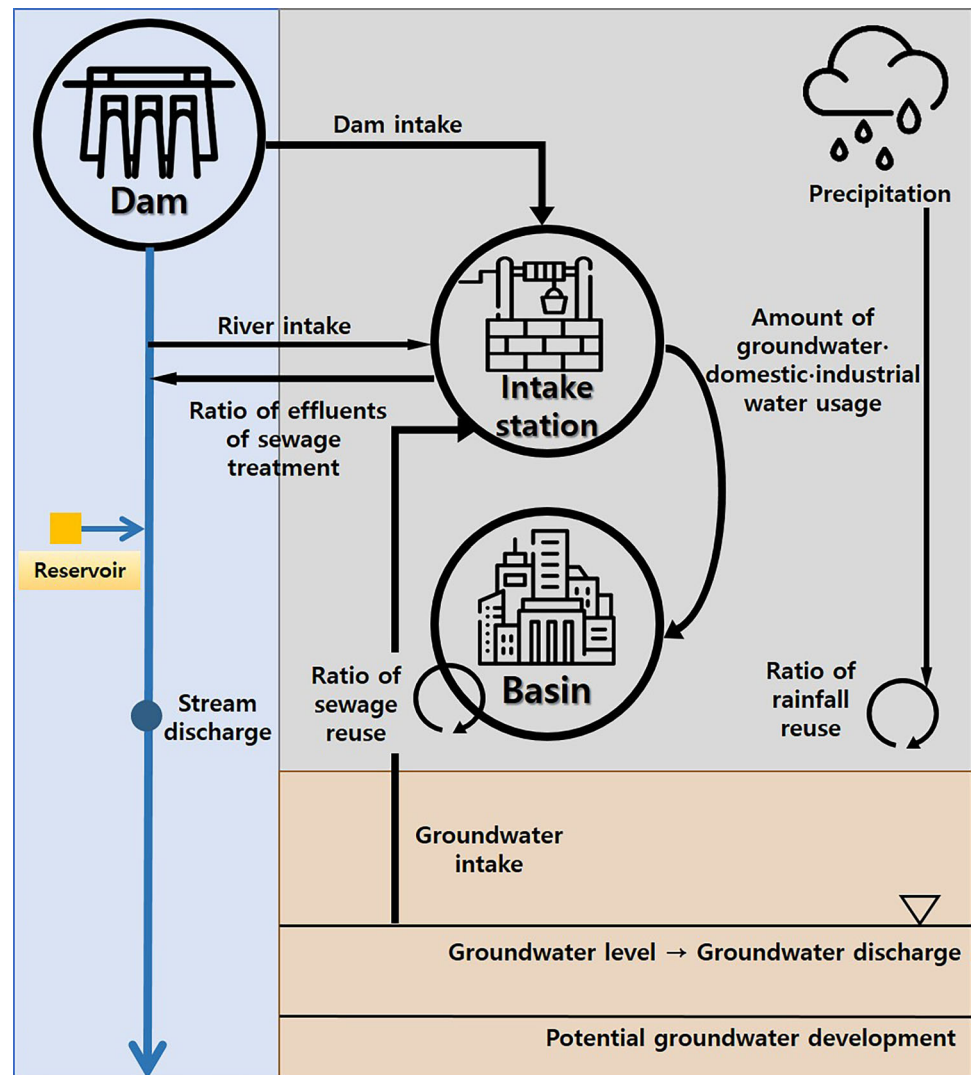**Fig. 5** Drought vulnerability map. **a** DVI$_{CDR}$, **b** DVI$_{MDR-RC}$

**Fig. 6** Diagram of the water supply system

The RC4 and RC5 districts have large populations but are rarely affected by droughts because of their abundant water supply. The northeast region, which includes the RC6 district, was generally rich in substitute resources such as groundwater. As a result, it had better drought response capacity. The results of this study are highly reflective of the regional characteristics of water supply and demand.

4.4 Drought risk assessment

In this study, CDR was defined as the potential damage and MDR-RC was defined as the potential damage linked with the water supply and demand. As shown in Fig. 8a, the DRI_{CDR} indicated that the R1, R2, and R3 districts were high, the risk in the southwest regions was generally high, and the R4, R5, and R6 districts had low risks. In contrast, the DRI_{MDR-RC} was highest in the R7, R8, and R9 districts, and generally high in the central and northeast regions, and the R10, R11, and R12 districts had low risks. There was a marked contrast between the DRI_{CDR} and the DRI_{MDR-RC}; the DRI_{CDR} was estimated only as DHI and DVI, and the DRI was therefore calculated due to the great influence of DHI, with a similar DVI for each region. However, the DRI_{MDR-RC} considered not only the DHI and DVI but also the DRCI, and the risk was estimated differently due to different vulnerable factors from region to region.

Comparing the drought risks with that of Kim et al. (2015), although the drought risk was markedly different depending on the purpose and indicators. The number of drought response measures, such as restrictions on water supply, is shown in Fig. 9 for comparison with areas that are actually at risk of drought. The data were limited by the short time-period for which they were collected and not representative of all drought impacts. However, they can be used to compare affected and non-affected districts, or to prioritize among affected districts. Figure 9 demonstrated that regions in the mid-west and northeast suffered the most drought damage. This result was similar to MDR-RC

Fig. 7 Drought response capacity map
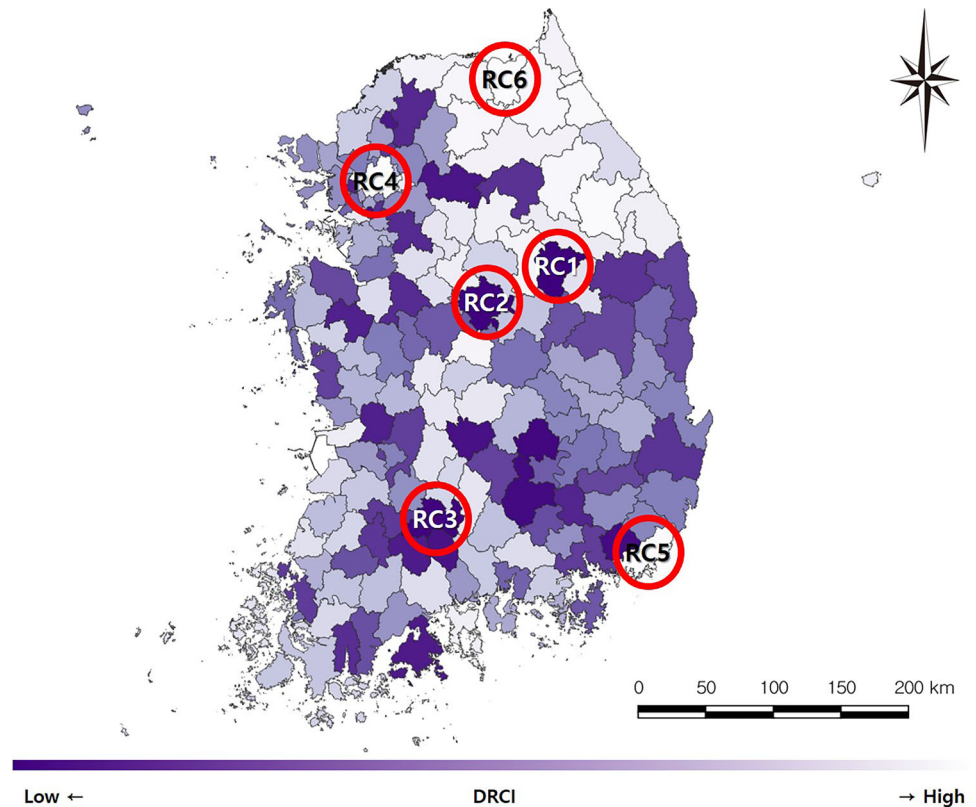
and different from CDR, where the southwest was at risk. It is confirmed that regions where the actual drought damage was severe are at high risk as MDR-RC reflects the water supply system. For MDR-RC, the west-central region was at risk in terms of hazard, vulnerability, and response capacity, while the northeast region was at high risk of hazard. Each region has different influencing factors and requires different drought response measures. MDR-RC was also valuable for quantifying patterns of drought due to water supply and demand. In the future, more extensive and reliable drought damage and impact data will improve the validity of the results.

5 Conclusion

Drought is intimately linked with communities and can be felt directly by humans. Calculating the drought risk without considering the water supply system does not accurately present actual drought risks. In this study, the modified drought risk coupled with response capacity considering the regional water supply system was assessed and compared with the conventional drought risk.

For drought hazard assessment, the DHI_{CDR} was high in the southern coastal regions, and the DHI_{MDR-RC} was high in the western coastal regions. In the western coastal regions, there were more drought forecasts and warnings than in the southern coastal regions. For drought vulnerability, the main attribute of the DVI_{CDR} was agricultural indicators, while the main attribute of the DVI_{MDR-RC} was the water supply indicators. However, drought vulnerabilities that were less affected by drought types were similarly high in inland regions. The drought response capacity was low in the southwest regions and the capacity to recover from drought was poor. Finally, for the drought risk assessment, the DRI_{CDR} was high in the southwest, and the DRI_{MDR-RC} was high in the central and northeast regions. The actual drought damage can be quantified by drought articles, drought forecasts, warnings, and restrictions of water supply, which are closely related to the regional water supply and demand. Although the regions identified by the DRI_{CDR} and DRI_{MDR-RC} were different, the regions of actual drought risk (the central and northeast regions) were identified by the DRI_{MDR-RC}.

We concluded that assessments of drought risk should consider the regional water supply system to ensure that local governments can cope with the regional impact of drought. The DRI_{MDR-RC} provides more detailed and accurate results in terms of water supply and demand compared with previous studies. The method used in this study provides a practical framework for obtaining information on drought impacts and risk related to water supply, which can be used for drought measures, strategies, decision making. This means that on the drought hazard side,

Fig. 8 Drought risk map.
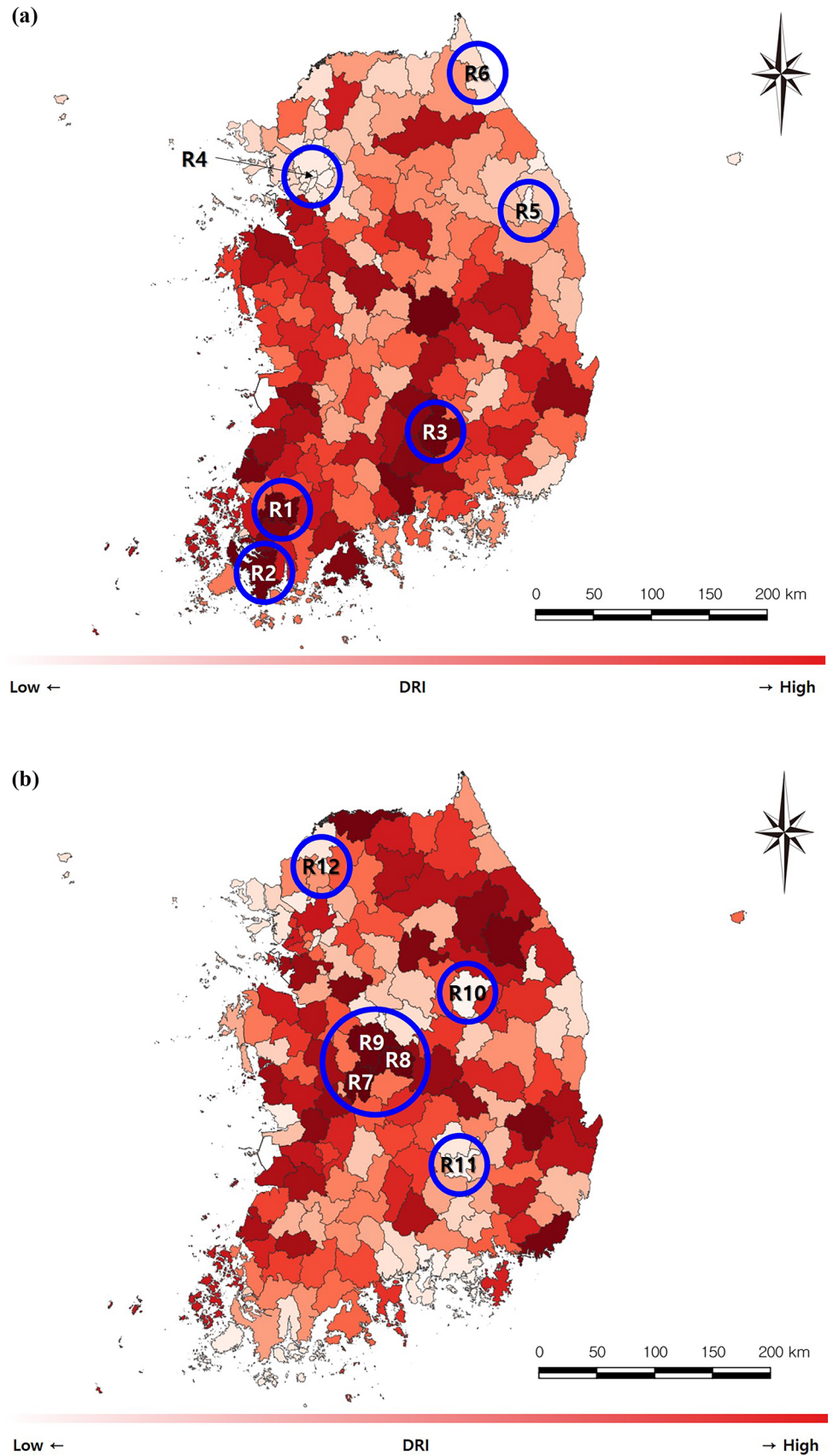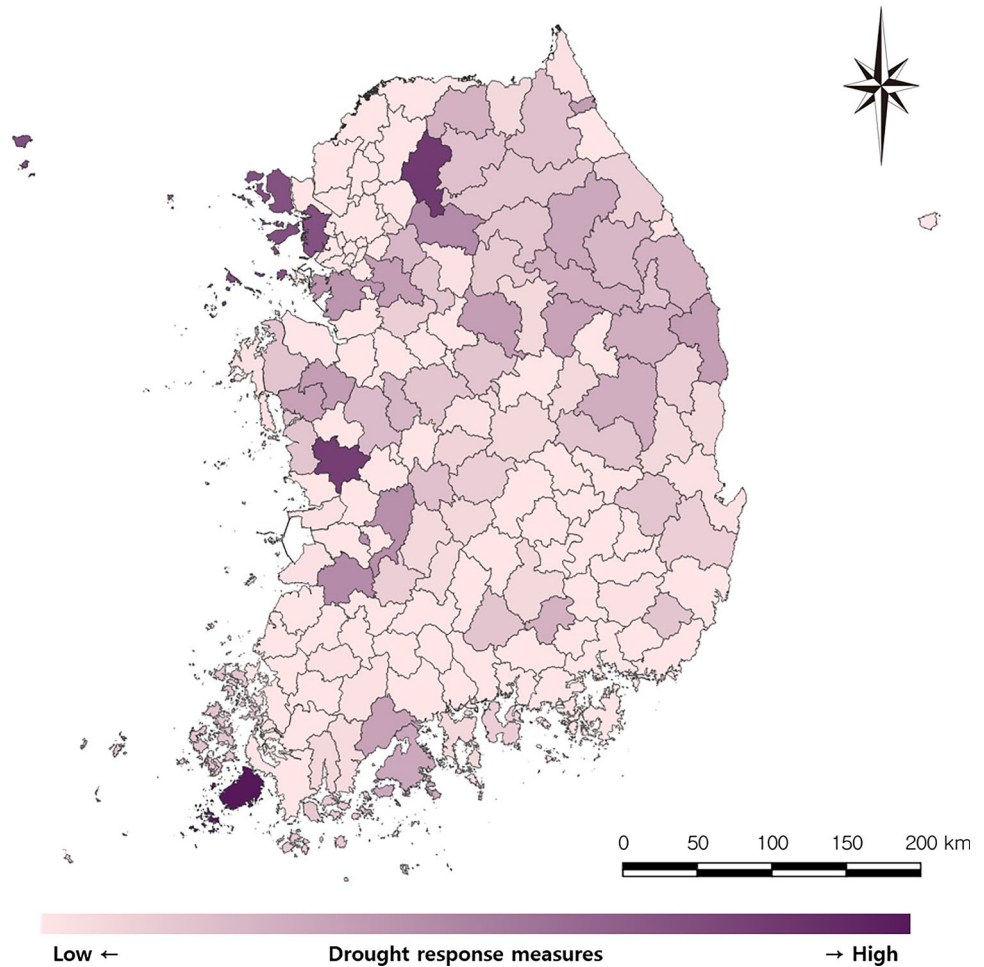**a** DRI$_{CDR}$, **b** DRI$_{MDR-RC}$

Fig. 9 Drought response measures

water supply failure events can be monitored based on the discharge. For the perspective of drought vulnerability, indicators affected by drought can be managed by suggesting policies for indicators with higher weighting. For the perspective of drought response capacity, it can compare supply adjustments and supplementary water sources to the ratio water supply against usage. This framework of regional drought risk assessment coupled with drought response capacity will help decision-makers plan for drought risk mitigation and prepare resource allocation strategies.

Our research has some limitations that can be addressed in further research. The factors are restricted in this study because we focused on methodology development and comparisons with existing methods. Different drought indices can consider both hydrometeorological droughts as well as water-related droughts. In the case of vulnerability and response capacity, additional data from national and local governments would be useful. In the process of selecting indicators, the quality of the model can be improved if objectivity supplied through PCA and

structural equation models. In addition, further research on drought risk mitigation measures utilizing drought response capabilities will enhance the applicability of this study.

Declarations

Conflict of interest The authors declared that they have no conflicts of interest to this work.

References

Azam M, Maeng SJ, Kim HS, Murtazaev A (2018) Copula-based stochastic simulation for regional drought risk assessment in South Korea. Water 10(4):359

Bae S, Lee SH, Yoo SH, Kim T (2018) Analysis of drought intensity and trends using the modified SPEI in South Korea from 1981 to 2010. Water 10(3):327

Birkmann J, Cardona OD, Carreño ML, Barbat AH, Pelling M, Schneiderbauer S, Kienberger S, Keiler M, Alexander D, Zeil P, Welle T (2013) Framing vulnerability, risk and societal responses: the MOVE framework. Nat Hazards 67(2):193-211

Brooks N, Adger WN, Kelly PM (2005) The determinants of vulnerability and adaptive capacity at the national level and the implications for adaptation. Glob Environ Chang 15:151–163

Buurman J, Bui DD, Du LTT (2020) Drought risk assessment in Vietnamese communities using household survey information. Int J Water Resour Dev 36(1):88–105

Cardona OD, Van Aalst MK, Birkmann J, Fordham M, McGregor G, Perez R, Pulwarty RS, Schipper ELF, Sinh BT (2012) Determinants of risk: exposure and vulnerability managing the risks of extreme events and disasters to advance climate change adaptation: special report of the intergovernmental panel on climate change. Cambridge University Press, New York, pp 65–108

Choi JR, Kim BS, Kang DH, Chung IM (2022) Evaluation of water supply capacity of a small forested basin water supply facilities using SWAT model and flow recession curve. KSCE J Civ Eng 26:3665–3675

Dabanli I (2018) Drought hazard, vulnerability, and risk assessment in Turkey. Arab J Geosci 11:538

Frischen J, Meza I, Rupp D, Wietler K, Hagenlocher M (2020) Drought risk to agricultural systems in Zimbabwe: a spatial analysis of hazard, exposure, and vulnerability. Sustainability 12(3):752

Hagenlocher M, Meza I, Anderson C, Min A, Renaud FG, Walz Y, Sebesvari Z (2019) Drought vulnerability and risk assessments: state of the art, persistent gaps, and research agenda. Environ Res Lett 14(8):083002

IPCC (2014) Climate change 2014: impacts, adaptation, and vulnerability. Part B: Regional aspects. Contribution of Working Group II to the Fifth Assessment Report of the Intergovernmental Panel on Climate Change. Cambridge University Press, New York

Kim CJ, Park MJ, Lee JH (2014) Analysis of climate change impacts on the spatial and frequency patterns of drought using a potential drought hazard mapping approach. Int J Climatol 34(1):61–80

Kim H, Park J, Yoo J, Kim TW (2015) Assessment of drought hazard, vulnerability, and risk: a case study for administrative districts in South Korea. J Hydro-Environ Res 9(1):28–35

Kim JS, Park SY, Hong HP, Chen J, Choi SJ, Kim TW, Lee JH (2020) Drought risk assessment for future climate projections in the Nakdong River Basin. Korea Int J Climatol 40(10):4528–4540

Kim JE, Yu JS, Ryu JH, Kim TW (2021) Assessment of regional drought vulnerability and risk using principal component analysis and a Gaussian mixture model. Nat Hazards 109:707–724

Liu A, Schisterman EF (2004) Principal component analysis. In: Chow S-C (ed) Encyclopedia of Biopharmaceutical Statistics. CPC Press, New York, pp 1796–1801

Mishra AK, Singh VP (2010) A review of drought concepts. J Hydrol 391(1–2):204–216

Moraru L, Moldovanu S, Dimitrievici LT, Dey N, Ashour AS, Shi F, Fong SJ, Khan S, Biswas A (2019) Gaussian mixture model for texture characterization with application to brain DTI images. J Adv Res 16:15–23

Murgatroyd A, Gavin H, Becher O, Coxon G, Hunt D, Fallon E, Wilson J, Cucelojlu G, Hall JW (2022) Strategic analysis of the drought resilience of water supply systems. Philos Trans Royal Soc 380(2238):20210292

Nam WH, Choi JY, Hong EM (2015) Irrigation vulnerability assessment on agricultural water supply risk for adaptive management of climate change in South Korea. Agric Water Manag 152:173–187

Nasrollahi M, Khosravi H, Moghaddamnia A, Malekian A, Shahid S (2018) Assessment of drought risk index using drought hazard and vulnerability indices. Arab J Geosci. https://doi.org/10.1007/s12517-018-3971-y

Qin QX, Zhang YB (2018) Evaluation and improvement of water supply capacity in the region. J Mgmt Sustainability 8(4):113–124

Rajsekhar D, Mishra AK, Singh VP (2012) Regionalization of drought characteristics using an entropy approach. J Hydrol Eng 18(7):870–887

Rajsekhar D, Singh VP, Mishra AK (2015) Integrated drought causality, hazard, and vulnerability assessment for future socioeconomic scenarios: an information theory perspective. J Geophys Res Atmos 120(13):6346–6378

Russell S, Norvig P (2009) Artificial intelligence: A modern approach, 3rd edn. Prentice Hall, Englewood Cliff, NJ

Shental N, Bar-Hillel A, Hertz T, Weinshall D (2004) Computing Gaussian mixture models with EM using equivalence constraints. Proc Adv Neural Inform Process Syst 16(8):465–472

Van Loon AF, Gleeson T, Clark J, Van Dijk AIJM, Stahl K, Hannaford J, Di Baldassarre G, Teuling AJ, Tallaksen LM, Uijlenhoet R, Hannah DM, Sheffield J, Svoboda M, Verbeiren B, Wagener T, Rangecroft S, Wanders N, Van Lanen HAJ (2016) Drought in the Anthropocene. Nat Geosci 9:89–91

Vogt JV, Naumann G, Masante D, Spinoni J, Cammalleri C, Erian W, Pischke F, Pulwarty R, Barbosa P (2018) Drought risk assessment and managemen: a conceptual framework. Publications Office of the European Union, Luxembourg

Wilhite DA (2000) Drought as a natural hazard: concepts and definitions. Routledge, New York, pp 3–18

Yoo J, Kwon HH, So BJ, Rajagopalan B, Kim TW (2015) Identifying the role of typhoons as drought busters in South Korea based on hidden Markov chain models. Geophys Res Lett 42(8):2797–2804

Yu J, Kim TW, Park DH (2019) Future hydrological drought risk assessment based on nonstationary joint drought management index. Water 11(3):532

Yu JS, Kim JE, Lee J-H, Kim T-W (2021) Development of a PCA-based vulnerability and copula-based hazard analysis for assessing regional drought risk. KSCE J Civ Eng 25(5):1901–1908

Zhao J, Zhang Q, Zhu X, Shen Z, Yu H (2020) Drought risk assessment in China: evaluation framework and influencing factors. Geography Sustainabil 1(3):220–228

Zhou R, Jin J, Cui Y, Ning S, Bai X, Zhang L, Zhou Y, Wu C, Tong F (2022) Agricultural drought vulnerability assessment and diagnosis based on entropy fuzzy pattern recognition and subtraction set pair potential. Alex Eng J 61(1):51–63

Zhu Y, Tian D, Yan F (2020) Effectiveness of entropy weight method in decision-making. Math Probl Eng 2020:1–5